

Dense Morphological Network: An Universal Function Approximator

Ranjan Mondal¹ Sanchayan Santra² Bhabatosh Chanda³

Abstract

Artificial neural networks are built on the basic operations comprising linear combination and non-linear activation function. Theoretically this structure can approximate any continuous function with three-layer architecture. The choice of activation function usually greatly influences the performance of the network. In this paper we propose the use of elementary morphological operations (dilation and erosion) as the basic operations in neurons. We show that the proposed network (called *DenMo-Net*) consisting of single layer of morphological neurons followed by a linear combination layer can approximate any smooth function. As DenMo-Net has an in-built non-linearity in the structure, no separate activation function is needed. But the use of max (resp. min) function in dilation (resp. erosion) results in optimization issues as the functions are only piecewise differentiable. To overcome this problem we have softened the min/max function to make it differentiable everywhere and, as a result, Soft DenMo-Net evolves. To best of our knowledge, this is the first work on network using dilation-erosion neurons, hence we focus only on the fully-connected layers. We have visually shown that the Soft DenMo-Net can classify circle data very accurately using only two morphological neurons. We have also evaluated our algorithm quantitatively on MNIST, Fashion-MNIST, SVHN, CIFAR-10 and HIGGS dataset. The results show that our network performs similarly well to similar structured neural network and some times better.

1. Introduction

In artificial neural networks, the basic building block is an artificial neuron or perceptron that simply computes the linear combination of the input (Rosenblatt, 1958). It is usually followed by a non-linear activation function to model the non-linearity of the output. Although the neurons are simple in nature, when connected together they can approximate any continuous function of the input (Hornik, 1991). This has been successfully utilized in solving different real world problems like image classification (Krizhevsky et al., 2012), semantic segmentation (Long et al., 2015) and image generation (Isola et al., 2017). While these models are quite powerful in nature, their efficient training can be hard in general (LeCun et al., 2012) and they need support of special techniques, such as batch normalization (Ioffe & Szegedy, 2015) and dropout (Srivastava et al., 2014), in order to achieve better generalization capabilities. Their training time also depends on the choice of activation function (Mishkin et al., 2017).

In this paper we are proposing new building blocks for building networks similar to neural network. Here, instead of the linear combination operation of the artificial neurons, we use a non-linear operation that eliminates the need of additional activation function while requiring a small number of neurons to attain same performance or better. More specifically, we use morphological operations (i.e. dilation and erosion) as the elementary operation of the neurons in the network. Our contribution in this paper is building a network with these operations that has the following properties.

1. Networks built with dilation-erosion neurons followed by linear combination can approximate any continuous function given enough dilation/erosion neurons.
2. As dilation and erosion operation are non-linear by themselves, requirement of separate non-linear activation function is eliminated.
3. The use of dilation-erosion operation greatly increases number of possible decision boundaries. As a result, complex decision boundaries can be learned using small number of parameters.
4. As an alternative to the max/min operation of dil-

¹Indian Statistical Institute, Kolkata, India ²Indian Statistical Institute, Kolkata, India ³Indian Statistical Institute, Kolkata, India. Correspondence to: ranjan15_r,sanchayan_r,chanda <@isical.ac.in>, sanchayan_r <@isical.ac.in>, chanda <@isical.ac.in>.

tion/erosion, using their soft version retains the above mentioned properties while making the operations differentiable.

The rest of the paper is organized as follows. Section 2 describes the prior work on morphological neural network. In Section 3, we introduce our proposed network and prove its capabilities theoretically. We further demonstrate its capabilities empirically on a few benchmark datasets in Section 4. Next, in Section 5 we have discussed about possible variants of our network, then concluding the paper in Section 6.

2. Related Work

Morphological neuron was first introduced by [Davidson & Hummer \(1993\)](#) in their effort to learn the structuring element of dilation operation in images. Similar effort has been made to learn the structuring elements in a more recent work by [Masci et al. \(2013\)](#). Use of morphological neurons in a more general setting was first proposed by [Ritter & Sussner \(1996\)](#). They restricted the network to a single layer architecture and focused only on binary classification task. To classify the data, these networks use two axis parallel hyperplanes as the decision boundary. This single layer architecture of [Ritter & Sussner \(1996\)](#) has been extended to two layer architecture by [Sussner \(1998\)](#). This two layer architecture is able to learn multiple axis parallel hyperplanes, and therefore is able to solve arbitrary binary classification task. But, in general the decision boundaries may not be axis parallel, as a result this two layer network may need to learn a large number of hyperplanes to achieve good results. So, one natural extension is to incorporate the option to rotate the hyperplanes. Taking a cue from this idea, [Barmoutis & Ritter \(2006\)](#) proposed to learn a rotational matrix that rotates the input before trying to classify the data using axis parallel hyperplanes. In a separate work by [Ritter et al. \(2014\)](#) the use of L^1 and L^∞ norm has been proposed as a replacement of the *max/min* operation of dilation and erosion in order to smooth the decision boundaries.

[Ritter & Urcid \(2003\)](#) first introduced the dendritic structure of biological neurons to the morphological neurons. This new structure creates hyperbox based decision boundaries instead of hyperplanes. The authors have proved that with hyperboxes any compact region can be estimated, therefore any two class classification problems can be solved. A generalization of this structure to the multiclass case has also been done by [\(Ritter & Urcid, 2007\)](#). [Sussner & Esmi \(2011\)](#) had proposed a new type of structure called morphological perceptrons with competitive neurons, where the output is computed in winner-take-all strategy. This is modelled using the *argmax* operator and this allows the network to learn more complex decision boundaries. Later [Sossa & Guevara \(2014\)](#) proposed a new training strategy to train

this model with competitive neurons.

The non-differentiability of the *max-min* operations has forced the researchers to propose specialized training procedures for their models. So, a separate line of research has attempted to modify these networks so that gradient descent based optimizer can be used for training. [Pessoa & Maragos \(2000\)](#) have combined the classical perceptron with the morphological perceptron. The output of each node is taken as the convex combination of the classical and the morphological perceptron. Although *max/min* operation is not differentiable, they have proposed methodology to circumvent this problem. They have shown that this network can perform complex classification tasks. Morphological neurons have also been employed for regression task. [de A. Arajo \(2012\)](#) has utilized network architecture similar to morphological perceptrons with competitive learning to forecast stock markets. The *argmax* operator is replaced with a linear function so that the network is able to regress forecasts. The use of linear activation function enables the use of gradient descent for training which is not possible with the *argmax* operator. For morphological neurons with dendritic structure [Zamora & Sossa \(2017\)](#) had proposed to replace the *argmax* operator with a softmax function. This overcomes the problem of gradient computation and therefore gradient descent is employed to train the network. So, this retains the hyperbox based boundaries of the dendritic networks, but facilitates easy training with gradient descent.

3. Dense Morphological Network

In this section we introduce the basic components and structure of our network and establish its approximation power.

3.1. Dilation and Erosion neurons

Dilation and Erosion are two basic operations of our proposed network. Given an input $\mathbf{x} \in \mathbb{R}^d$ and some structuring element $\mathbf{s} \in \mathbb{R}^{d+1}$, **dilation** (\oplus) and **erosion** (\ominus) neurons computes the following two functions respectively

$$\mathbf{x} \oplus \mathbf{s} = \max_k (x'_k + s_k), \quad (1)$$

$$\mathbf{x} \ominus \mathbf{s} = \min_k (x'_k - s_k). \quad (2)$$

Where $\mathbf{x}' = [\mathbf{x}, 0]$ and x'_k denotes the k^{th} component of vector \mathbf{x}' . The 0 is appended to the input \mathbf{x} to take care of the ‘bias. The only parameter that involves in this morphological operation is (\mathbf{s}). Note that erosion operation can also be written in the following form.

$$\mathbf{x} \ominus \mathbf{s} = - \max_k (s_k - x'_k) \quad (3)$$

3.2. Network Structure

The Dense Morphological Net or ‘DenMo-Net’, in short, that we propose here is a simple feed forward network with

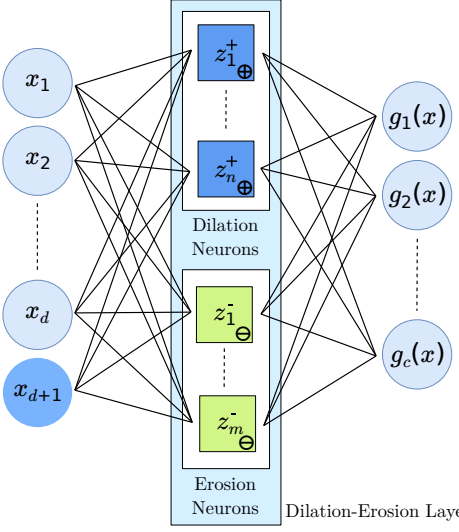


Figure 1. Architecture of single layer DenMo-Net. It contains an input layer, a dilation-erosion layer and a linear combination layer at the end. The dilation-erosion layer contains n dilation and m erosion neuron, and c neurons in the linear combination layer that also serves as the output layer.

some dilation and erosion neurons followed by linear combination (Figure 1). We call the layer of dilation and erosion neurons as the **dilation-erosion layer** and the following layer as the **linear combination layer**. Let's assume the dilation-erosion layer contains n dilation neurons and m erosion neurons, followed by c neurons in the linear combination layer. Let $\mathbf{x} \in \mathbb{R}^d$ is the input to the network. Let z_i^+ and z_j^- be the output of i^{th} dilation neuron and j^{th} erosion node, respectively. Then we can write,

$$z_i^+ = \mathbf{x} \oplus \mathbf{s}_i^+, \quad (4)$$

$$z_j^- = \mathbf{x} \ominus \mathbf{s}_j^- \quad (5)$$

where, \mathbf{s}_i^+ and \mathbf{s}_j^- are the structuring elements of the i^{th} dilation neuron and j^{th} erosion neuron respectively. Note that $i \in \{1, 2, \dots, n\}$ and $j \in \{1, 2, \dots, m\}$. The final output from a node of the linear combination layer is computed in the following way,

$$g(\mathbf{x}) = \sum_{i=1}^n z_i^+ \omega_i^+ + \sum_{j=1}^m z_j^- \omega_j^- \quad (6)$$

where ω_i^+ and ω_j^- are the weights of the artificial neuron in the linear combination layer. In following subsection we show that $g(\mathbf{x})$ can approximate any continuous function $f : \mathbb{R}^d \rightarrow \mathbb{R}$.

3.3. Function Approximation

Here we show that with the linear combination of dilation and erosion, any function can be approximated, and the

approximation error decreases with increase in the number of neurons in the dilation-erosion layer. Before that we need to describe some concepts.

Definition 1 (k -order Hinge Function) (Wang & Sun, 2005) A k -order hinge function consists of $(k+1)$ hyperplanes continuously joined together. it is defined by the following equation,

$$h^{(k)}(\mathbf{x}) = \pm \max\{\mathbf{w}_1^T \mathbf{x} + b_1, \mathbf{w}_2^T \mathbf{x} + b_2, \dots, \mathbf{w}_{k+1}^T \mathbf{x} + b_{k+1}\}. \quad (7)$$

Definition 2 (d -order hinging hyperplanes (d -HH)) (Wang & Sun, 2005) A d -order hinging hyperplanes (d -HH) is defined as the sum of multi-order hinge function as follows,

$$\sum_i \alpha_i h^{(k_i)}(\mathbf{x}) \quad (8)$$

with $\alpha_i \in \{-1, 1\}$, $k_i \leq d$.

From Wang & Sun (2005) the following can be said about hinging hyperplanes.

Proposition 1 For any given positive integer d and arbitrary continuous piece-wise linear function $f : \mathbb{R}^d \rightarrow \mathbb{R}$, there exists finite, say N , positive integers $\eta(k) \leq d+1$, $1 \leq k \leq N$ and corresponding $\alpha_i \in \{-1, 1\}$ such that

$$f(\mathbf{x}) = \sum_{k=1}^N \alpha_i h^{(\eta(k))}(\mathbf{x}), \quad \forall \mathbf{x} \in \mathbb{R}^d. \quad (9)$$

This says that any continuous piece-wise linear function of d variables can be written as an d -HH, i.e. the sum of multi-order hinge functions. Now to show that our network can approximate any continuous functions, we show the following.

Lemma 1 $g(\mathbf{x})$ is sum of multi-order hinge functions.

The proof of this lemma is given in the supplementary document. There we show that $g(\mathbf{x})$ can be written as the sum of l hinge functions in the following form.

$$g(\mathbf{x}) = \sum_{i=1}^l \alpha_i \phi_i(\mathbf{x}) \quad (10)$$

where $l = m+n$ (number of neurons in the dilation-erosion layer), $\alpha_i \in \{1, -1\}$ and $\phi_i(\mathbf{x})$'s are d -order hinge function.

Proposition 2 (Stone-Weierstrass approximation theorem)

Let C be a compact domain ($C \subset \mathbb{R}^d$) and $f : C \rightarrow \mathbb{R}$ a continuous function. Then there exists a continuous piece wise linear function g such that for all $\mathbf{x} \in C$, $|f(\mathbf{x}) - g(\mathbf{x})| < \epsilon$ for some $\epsilon > 0$.

Theorem 1 (Universal approximation) Only a single dilation-erosion layer followed by a linear combination layer can approximate any continuous smooth function provided there are enough nodes in dilation erosion-layer.

Sketch of Proof From lemma 1 we know that our DenMo-Net with of n dilation and m erosion neurons followed by a linear combination layer computes $g(x)$, which is a sum of multi-order hinge functions. Now from proposition 1 we get that any continuous piecewise linear function can be written by a finite sum of multi-order hinge function. Now from Proposition 2 we can say that any continuous function can be well approximated by a piecewise linear function. In general if $l \rightarrow \infty$ then $\epsilon \rightarrow 0$. If we increase the number of neurons in the dilation-erosion layer the approximation error decreases. Therefore, we can say that a DenMo-Net with enough dilation and erosion neurons can approximate any continuous function.

3.4. Learned Decision Boundary

The DenMo-Net we have defined above learns the following function,

$$g(\mathbf{x}) = \sum_{i=1}^l \alpha_i \phi_i(\mathbf{x}). \quad (11)$$

Where each $\phi(\mathbf{x})$ is collection of multiple hyperplanes joined together. Therefore the number of hyperplanes learned by the network with l neurons in the dilation-erosion layer is much more than l . Each morphological neuron allows only one of the inputs to pass through because of max / min operation after addition with the structuring element. So, effectively each neuron in the dilation-erosion layer chooses one component of the d -dimensional input vector. Depending on which component is being chosen, the final linear combination layer computes the hyperplane by taking either all the components of the input or only some of them (when a subset of input components is chosen more than once in the dilation-erosion layer). Note that this choice depends on the input and the structuring element together. For a network with d dimensional input data and l neurons ($l \geq d$) in the dilation-erosion layer, theoretically maximum $(d+1)^l - 1$ hyperplanes can be formed in d dimension. Out of the all possible planes only ${}^l P_d \times (d+1)^{l-d}$ planes can span anywhere in the d dimensional space. Therefore, increasing the number of neurons in the dilation-erosion layer exponentially increases the possible number of hyperplanes, i.e., the decision boundaries. This implies that, using only a small number of neurons, complex decision boundaries can be learned.

3.5. Soft DenMo-Net

Morphological neurons, i.e dilation and erosion neurons use max and min operation respectively. max and min

operations are piecewise differentiable. However while back propagation from a single morphological neurons, only a single value of structuring elements is updated due to max and min operation. To get smooth approximation of max and min we follow Cook (2011) and redefine dilation and erosion operation by the following.

$$\mathbf{x} \oplus s = \log\left(\sum_k e^{(x'_k + s_k)\beta}\right)/\beta \quad (12)$$

$$\mathbf{x} \ominus s = -\log\left(\sum_k e^{(s_k - x'_k)\beta}\right)/\beta \quad (13)$$

Where β is the "hardness" of the soft maximum. In general, if $\beta \rightarrow \infty$ then equation 12 and equation 13 converges to equation 1 and equation 2 respectively. However, taking very high value of β may overflow the 32 bit floating point variable.

Please see the supplementary material for the proof. We call the network with soft dilation and soft erosion as Soft DenMo-Net.

4. Results

Here we empirically evaluate the performance of DenMo-Net and Soft DenMo-Net and demonstrate their advantages.

4.1. Baseline

As we have defined our network with 1D structuring elements, we compare our method with similar structured fully connected neural network with various activation functions, like tanh (NN-tanh) and ReLU (NN-ReLU) and Maxout network (Goodfellow et al., 2013). We have particularly chosen the maxout network for comparison, because it uses the *max* function as a replacement of the activation function but with added nodes to compute the maximum. The experiments have been carried out on benchmark datasets like MNIST (LeCun et al., 1998), Fashion-MNIST (Xiao et al., 2017), SVHN (Netzer et al., 2011), CIFAR-10 and Higgs (Baldi et al., 2014). However, at the beginning experiment is carried out on a toy dataset consisting of data approximately on two concentric circles for visualizing the decision boundaries. In our experiment with benchmark image datasets, each image data is flattened in row major order before it is fed into the network. So, network is unaware of the spatial structure of image. For all the tasks we have used categorical cross entropy as the loss and in the last layer softmax function is used. In the training phase, network is optimized using Adam optimizer (learning rate=0.001, $\beta_1=0.9$, $\beta_2=0.999$) (Kingma & Ba, 2014). We have used glorot uniform initialization (Glorot & Bengio, 2010) for initializing all the structuring elements and weights of neural network. We have initialized all the bias to zero. We

Table 1. Training accuracy achieved on the circle dataset by different networks using only two hidden neurons.

Methods	# Parameters	Training accuracy
NN-ReLU	12	69.30
Maxout Network (h=2)	18	90.02
DenMo-Net	12	94.10
Soft DenMo-Net($\beta = 3$)	12	97.3

have used same number of dilation (resp. erosion) neurons in dilation (resp. erosion) layer unless otherwise stated.

4.2. Visualization with a toy dataset

For visualizing the decision boundaries learned by the classifiers, we have generated data on two concentric circles belonging to two different classes with center at the origin. We compare the results when only two neurons are taken in the hidden layer in all the networks. It is observed that baseline neural network fails to classify this data with two hidden neurons as it learns one hyperplane per one hidden neuron. The boundaries learned by the network with ReLU activation function (NN-ReLU) is shown in figure 2a. The result of maxout network is better (90.02% training accuracy) in this case, as it introduces extra parameters with max function to achieve non-linearity. In the maxout layer we have taken maximum among $h = 2$ features. As we see in the figure 2b the network learns $(2 * h =) 4$ hyper planes when trying to classify these data. For the same data and two morphological neurons in dilation-erosion layer, our DenMo-Net has learned 6 lines to form the decision boundary (figure 2c). Although from equation 11 we can say that we can get at most 8 distinct lines, only two of them can be placed anywhere in the 2D space while others are parallel to the axes. For this reason, we are getting two slanted lines and the remaining lines are parallel to the axes.

We have also shown the decision boundary learned by Soft DenMo-Net (figure 2d). We have taken hardness constant $\beta = 3$ for Soft DenMo-Net. We see that the decision boundary learned by Soft DenMo-Net are smooth, hence it get perfect decision boundary in circle data, with only two hidden morphological neurons.

The classification accuracy achieved by the networks along with their number of parameters is reported in Table 1. The accuracy clearly reveals the efficacy of DenMo-Net.

4.3. Experiment on MNIST Dataset

MNIST dataset (LeCun et al., 1998) contains gray scale images of hand written numbers (0-9) of size 28×28 . It has 60,000 training images and 10,000 test images. Since our network is defined on one dimensional input, we have converted each image to a column vector (in row major order) before using it as input. The network we use follows the

Table 2. Achieved accuracy in the test on MNIST and Fashion-MNIST Dataset using a single hidden layer Network with 400 hidden morphological neurons.

Dataset	Test Accuracy		
	DenMo-Net	Soft DenMo-Net ($\beta = 8$)	State-of-the-art
MNIST	98.39	98.90	(Wan et al., 2013)
Fashion-MNIST	89.87	89.70	(Xiao et al., 2017)

structure we have previously defined: input layer, dilation-erosion layer and linear combination layer computing the output. As in this dataset we had to distinguish between 10 classes of images, 10 neurons are taken in the output layer. In Table 2 we have shown the accuracy on test data after training the network for 150 epochs with different number of nodes (l) in the dilation-erosion layer. We get average test accuracy of 98.39% and 98.90% after training 3 times with the DenMo-Net and Soft DenMo-Net ($\beta = 8$) respectively with 200 dilation and 200 erosion neurons (Table 2) up to 400 epochs. However, it maybe noted that, better pre-processing of data may result higher accuracy.

4.4. Experiment on Fashion-MNIST Dataset

The Fashion-MNIST dataset (Xiao et al., 2017) has been proposed with the aim of replacing the popular MNIST dataset. Similar to the MNIST dataset this also contains 28×28 images of 10 classes and 60,000 training and 10,000 testing samples. While MNIST is still a popular choice for benchmarking classifiers, the authors' claim that MNIST is too easy and does not represent the modern computer vision tasks. This dataset aims to provide the accessibility of the MNIST dataset while posing a more challenging classification task. For the experiment, we have converted the images to a column vector similar to what we have done for the MNIST dataset. We have taken 250 dilation and 250 erosion nodes in the dilation-erosion layer for this experiment. The only pre-processing we have done is normalized the data between [0,1]. We have trained the network separately 3 times up to 300 epochs. The reported test accuracy (Table 2) is the average of the 3 runs. We see that our method gives comparable results with the state-of-the-art.

4.5. Experiment on SVHN Dataset

Street View House Numbers (SVHN) dataset (Netzer et al., 2011) is similar to MNIST dataset in the sense both of them contains images of numerals written in english. In this dataset the images are collected from house numbers in

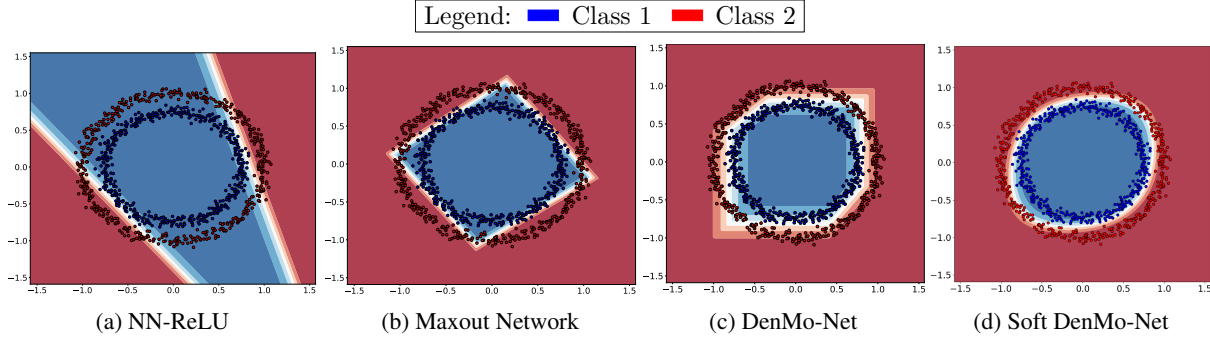


Figure 2. Decision boundaries learned by different networks with two hidden neurons. Normal neural network is able to learn only two planes (figure 2a). Maxout networks (figure 2b) is able to learn two more planes with the help of additional parameters. DenMo-Net is able to learn more planes with same number of parameters as NN-ReLU (figure 2c). Using soft version of DenMo-Net, smooths the learned decision boundary (figure 2d). This further enhances the discrimination capability of the network while retaining the same number of parameters.

Table 3. Test accuracy achieved on CIFAR-10 dataset by different networks, varying number of neurons(l) in the hidden layer

Architecture	l=200		l=400		l=600	
	parameters	accuracy	parameters	accuracy	parameters	accuracy
NN-tanh	616,610	49.22	1,233,210	51.02	1,849,810	52.18
NN-ReLU	616,610	48.89	1,233,210	51.66	1,849,810	51.57
Maxout-Network	1,231,210	50.87	2,462,410	51.12	3,693,610	52.19
DenMo-Net	616,610	51.81	1,233,210	54.13	1,849,810	54.60
Soft DenMo-Net($\beta = 12$)	616,610	52.52	1,233,210	54.58	1,849,810	55.59

Table 4. Test accuracy achieved on SVHN dataset by different networks, varying number of neurons(l) in the hidden layer

Architecture	l=200		l=400		l=600	
	parameters	accuracy	parameters	accuracy	parameters	accuracy
NN-tanh	616,610	75.24	1,233,210	76.72	1,849,810	77.28
NN-ReLU	616,610	68.26	1,233,210	75.46	1,849,810	77.33
Maxout-Network	1,231,210	68.12	2,462,410	71.85	3,693,610	75.59
DenMo-Net	616,610	71.87	1,233,210	75.95	1,849,810	77.80
Soft DenMo-Net($\beta = 20$)	616,610	73.07	1,233,210	75.68	1,849,810	78.24

Google Street View images. Like MNIST all the images are 32×32 centered on a single character. But unlike MNIST, here the images are not grayscale. They are color images. The dataset has around 73257 training samples and 26032 test samples. For the experiment we have flattened the image in row major order and normalized between [0,1]. In Table 4 we have reported the test accuracy achieved by different networks along with their number of parameters. We see that even with increased number of parameters is performing the poorest. On the other hand both DenMo-Net and Soft DenMo-Net perform close to the best performing classifier.

4.6. Experiment on CIFAR-10 Dataset

CIFAR-10 (Krizhevsky & Hinton, 2009) is natural image dataset with 10 classes. It has 50,000 training and 10,000 test images. Each of them is a color image of size 32×32 . The images are converted to column vector before they are fed to the DenMo-Net. For all the networks we compare with, the experiments have been conducted keeping the number of neurons same in the hidden layer. Note that, in maxout network, each hidden neuron has two extra nodes over which the maximum is computed. In Table 3 we have reported the average test accuracy obtained over three runs of 150 epochs. It can be seen from the table that DenMo-Net achieves the best accuracy in all the cases. Maxout network lags behind even with more number of parameters. This happens because our network is able to learn more hyperplanes with number of parameters similar to standard artificial neural networks. However, using only a single type of morphological neurons in our network, we get a different result for this dataset (Figure 3). Soft DenMo-Net ($\beta = 20$) achieves accuracy of 59.21% using 1200 morphological neurons.

4.7. Higgs Dataset

Higgs Dataset (Baldi et al., 2014) is built to benchmark the performance of neural networks in distinguishing signal process producing Higgs boson from the background process that does not. This is a synthetically generated dataset with 28 features commonly used by the physicists to distinguishing between the two. The dataset has 11 million data instances. Out of which we have taken random 80% as the training data and rest as the test data. The features have been normalized between -1 and 1 before they are sent to training. In Table 5, We have reported the performance of the network. We see that DenMo-Net performs better than Soft DenMo-Net. However the performance with other network are very similar.

Table 5. Test accuracy achieved on Higgs dataset

Architecture(l=200)	Accuracy
DenMo-Net	73.23
Soft DenMo-Net($\beta = 20$)	72.84
NN-tanh	71.20
NN-Relu	74.34
NN-Maxout	74.88

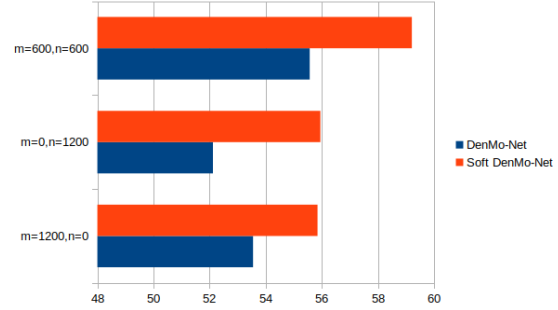


Figure 3. Accuracy of CIFAR10 dataset. m and n denotes the number of dilation and erosion neurons respectively in the dilation-erosion layer. The performance of both DenMo-Net and Soft DenMo-Net gets better when both dilation and erosion neurons are used.

5. Discussions

5.1. Ablation Study

Theoretically DenMo-Net can act as an universal approximator with only dilation (or erosion) neurons. But in practice, presence of both dilation and erosion neurons in the dilation-erosion layer improves performance. To empirically justify this claim we have taken the help of CIFAR-10 dataset. We have reported the change in test accuracy over the epochs for DenMo-Net and Soft DenMo-Net in figure 4 and figure 5 respectively. In the experiments with both the networks the total number of neurons in the dilation-erosion layer has been kept the same (1200). In both the cases, we see the use of both types of nodes results in a jump in the performance, which is not attained even after several epochs when using one type of neurons only.

5.2. Stacking Multiple Layers

We have defined the network and have shown its properties when only three layers are employed in the network. Straight-forward stacking of the layers that we may use in our network can give rise to two kinds of network.

Type-I Multiple dilation-erosion layer followed by a single linear combination layer at the end.

Type-II Unit formed by a Dilation-Erosion layer followed by a linear combination layer repeated multiple times.

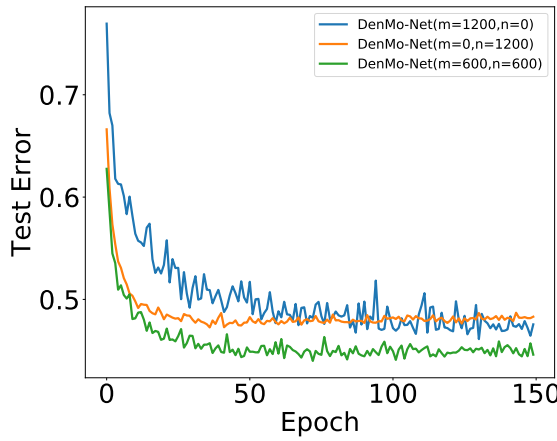


Figure 4. Epochs vs test error in CIFAR10 dataset with DenMo-Net containing 1200 hidden neurons. using both type of neurons the network surpassed the classification accuracy that is achieved when using a single type of neuron.

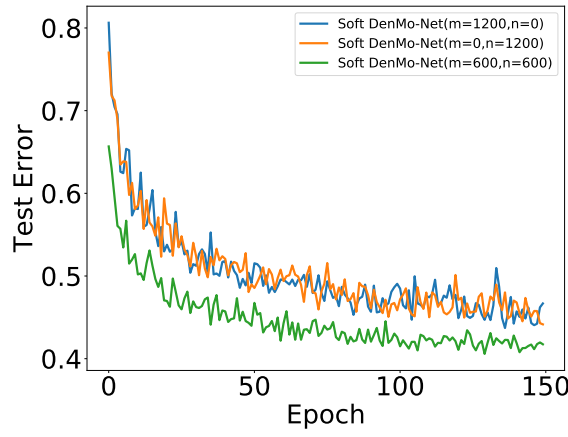


Figure 5. Epochs vs test error in CIFAR10 dataset with Soft DenMo-Net containing 1200 hidden neurons. Use of both type of neurons is adding to the improved classification accuracy by a significant margin.

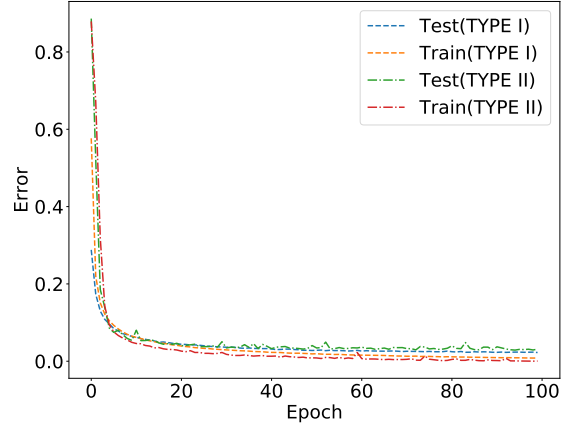


Figure 6. Epochs vs training and test error in MNIST dataset with network architecture 200DE-200FC-200DE-10FC (Type-I) and 200DE-200FC-200DE-10FC(Type-II). Both network performs similar to single hidden layer DenMo-Net

For the network of Type-I, it can be argued that the network is performing some concatenation of opening and closing operations and, finally, their linear combination. As there are dilation-erosion (DE) layers back to back, the problem of gradient propagation is amplified. As a result it takes much more time to train compared to single layer architecture (figure 7).

Similar explanation doesn't hold good for Type-II networks. Type-II gives similar results as single hidden layer DenMo-Net as shown in figure 6 and figure 7. However, in cifar10, It highly overfits. We believe its understanding requires further exploration and extension towards 2D Morphological network which takes 2D image as input.

6. Conclusion

In this paper we have proposed a new class of networks that uses morphological neurons. These network consists of three layers only: input layer, dilation-erosion layer followed by linear combination layer giving the output of the network. We have presented analysis using this three layer network only, but its deeper version should be explored in future. We have shown that unlike standard Artificial Neural Network this proposed three layer architecture can approximate any smooth function without any activation function provided there are enough dilation, erosion neurons. Second, these proposed networks are able to learn a large number of hyper-planes with very few neurons in the dilation-erosion layer and thereby provide superior results compared to other networks with three layer architecture. In this work we have only worked with fully connected layers, i.e. a node in a layer is connected to all the nodes in the previous layer. This type of connectivity is not very efficient for image data

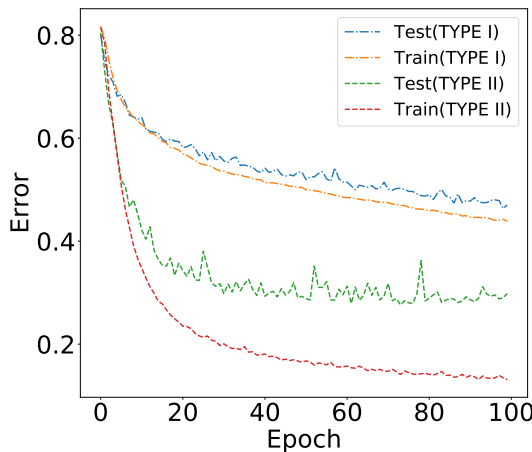


Figure 7. Epochs vs training and test error in SVHN dataset with network architecture 200DE-200FC-200DE-10FC (Type-I) and 200DE-200FC-200DE-10FC (Type-II). Network of Type-I converges slowly than the network of Type-II.

where architectures with convolution layers perform better. So, extending this work to the case where a structuring element operates by sliding over the whole image, should be the next logical step.

References

Baldi, P., Sadowski, P., and Whiteson, D. Searching for exotic particles in high-energy physics with deep learning. *Nature communications*, 5:4308, 2014.

Barmpoutis, A. and Ritter, G. X. Orthonormal Basis Lattice Neural Networks. In *2006 IEEE International Conference on Fuzzy Systems*, pp. 331–336, July 2006. doi: 10.1109/FUZZY.2006.1681733.

Cook, J. D. Basic properties of the soft maximum. *UT MD Anderson Cancer Center Department of Biostatistics Working Paper Series; Working Paper 70*, 2011.

Davidson, J. L. and Hummer, F. Morphology neural networks: An introduction with applications. *Circuits, Systems and Signal Processing*, 12(2):177–210, June 1993. ISSN 1531-5878. doi: 10.1007/BF01189873.

de A. Arajo, R. A morphological perceptron with gradient-based learning for Brazilian stock market forecasting. *Neural Networks*, 28:61–81, April 2012. ISSN 0893-6080. doi: 10.1016/j.neunet.2011.12.004.

Glorot, X. and Bengio, Y. Understanding the difficulty of training deep feedforward neural networks. In *Proceedings of the thirteenth international conference on artificial intelligence and statistics*, pp. 249–256, 2010.

Goodfellow, I. J., Warde-Farley, D., Mirza, M., Courville, A., and Bengio, Y. Maxout Networks. In *Proceedings of the 30th International Conference on International Conference on Machine Learning - Volume 28*, ICML’13, pp. III–1319–III–1327, Atlanta, GA, USA, 2013. JMLR.org.

Hornik, K. Approximation capabilities of multilayer feedforward networks. *Neural Networks*, 4(2):251–257, January 1991. ISSN 0893-6080. doi: 10.1016/0893-6080(91)90009-T.

Ioffe, S. and Szegedy, C. Batch Normalization: Accelerating Deep Network Training by Reducing Internal Covariate Shift. In *International Conference on Machine Learning*, pp. 448–456, June 2015.

Isola, P., Zhu, J., Zhou, T., and Efros, A. A. Image-to-Image Translation with Conditional Adversarial Networks. In *2017 IEEE Conference on Computer Vision and Pattern Recognition (CVPR)*, pp. 5967–5976, July 2017. doi: 10.1109/CVPR.2017.632.

Kingma, D. P. and Ba, J. Adam: A Method for Stochastic Optimization. *arXiv:1412.6980 [cs]*, December 2014. arXiv: 1412.6980.

Krizhevsky, A. and Hinton, G. Learning multiple layers of features from tiny images. Technical report, University of Toronto, 2009.

Krizhevsky, A., Sutskever, I., and Hinton, G. E. ImageNet Classification with Deep Convolutional Neural Networks. In Pereira, F., Burges, C. J. C., Bottou, L., and Weinberger, K. Q. (eds.), *Advances in Neural Information Processing Systems 25*, pp. 1097–1105. Curran Associates, Inc., 2012.

LeCun, Y., Bottou, L., Bengio, Y., and Haffner, P. Gradient-based learning applied to document recognition. *Proceedings of the IEEE*, 86(11):2278–2324, 1998.

LeCun, Y. A., Bottou, L., Orr, G. B., and Müller, K.-R. Efficient BackProp. In Montavon, G., Orr, G. B., and Müller, K.-R. (eds.), *Neural Networks: Tricks of the Trade: Second Edition*, Lecture Notes in Computer Science, pp. 9–48. Springer Berlin Heidelberg, Berlin, Heidelberg, 2012. ISBN 978-3-642-35289-8. doi: 10.1007/978-3-642-35289-8_3.

Long, J., Shelhamer, E., and Darrell, T. Fully convolutional networks for semantic segmentation. In *2015 IEEE Conference on Computer Vision and Pattern Recognition (CVPR)*, pp. 3431–3440, June 2015. doi: 10.1109/CVPR.2015.7298965.

Masci, J., Angulo, J., and Schmidhuber, J. A learning framework for morphological operators using counter-harmonic mean. In *International Symposium on Mathematical Morphology and Its Applications to Signal and Image Processing*, pp. 329–340. Springer, 2013.

Mishkin, D., Sergievskiy, N., and Matas, J. Systematic evaluation of convolution neural network advances on the Imagenet. *Computer Vision and Image Understanding*, 161:11–19, August 2017. ISSN 1077-3142. doi: 10.1016/j.cviu.2017.05.007.

Netzer, Y., Wang, T., Coates, A., Bissacco, A., Wu, B., and Ng, A. Y. Reading digits in natural images with unsupervised feature learning. In *NIPS workshop on deep learning and unsupervised feature learning*, volume 2011, pp. 5, 2011.

Pessoa, L. F. C. and Maragos, P. Neural networks with hybrid morphological/rank/linear nodes: a unifying framework with applications to handwritten character recognition. *Pattern Recognition*, 33(6):945–960, June 2000. ISSN 0031-3203. doi: 10.1016/S0031-3203(99)00157-0.

Ritter, G. X. and Sussner, P. An introduction to morphological neural networks. In *Proceedings of 13th International Conference on Pattern Recognition*, volume 4, pp. 709–717 vol.4, August 1996. doi: 10.1109/ICPR.1996.547657.

Ritter, G. X. and Urcid, G. Lattice algebra approach to single-neuron computation. *IEEE Transactions on Neural Networks*, 14(2):282–295, March 2003. ISSN 1045-9227. doi: 10.1109/TNN.2003.809427.

Ritter, G. X. and Urcid, G. Learning in Lattice Neural Networks that Employ Dendritic Computing. In Kaburlasos, V. G. and Ritter, G. X. (eds.), *Computational Intelligence Based on Lattice Theory*, Studies in Computational Intelligence, pp. 25–44. Springer Berlin Heidelberg, Berlin, Heidelberg, 2007. ISBN 978-3-540-72687-6. doi: 10.1007/978-3-540-72687-6_2.

Ritter, G. X., Urcid, G., and Juan-Carlos, V. Two lattice metrics dendritic computing for pattern recognition. In *2014 IEEE International Conference on Fuzzy Systems (FUZZ-IEEE)*, pp. 45–52, July 2014. doi: 10.1109/FUZZ-IEEE.2014.6891551.

Rosenblatt, F. The perceptron: A probabilistic model for information storage and organization in the brain. *Psychological Review*, 65(6):386–408, 1958. ISSN 1939-1471(Electronic),0033-295X(Print). doi: 10.1037/h0042519.

Sossa, H. and Guevara, E. Efficient training for dendrite morphological neural networks. *Neurocomputing*, 131: 132–142, May 2014. ISSN 0925-2312. doi: 10.1016/j.neucom.2013.10.031.

Srivastava, N., Hinton, G., Krizhevsky, A., Sutskever, I., and Salakhutdinov, R. Dropout: a simple way to prevent neural networks from overfitting. *The Journal of Machine Learning Research*, 15(1):1929–1958, 2014.

Sussner, P. Morphological perceptron learning. In *Proceedings of the 1998 IEEE International Symposium on Intelligent Control (ISIC) held jointly with IEEE International Symposium on Computational Intelligence in Robotics and Automation (CIRA) Intell*, pp. 477–482, September 1998. doi: 10.1109/ISIC.1998.713708.

Sussner, P. and Esmi, E. L. Morphological perceptrons with competitive learning: Lattice-theoretical framework and constructive learning algorithm. *Information Sciences*, 181(10):1929–1950, May 2011. ISSN 0020-0255. doi: 10.1016/j.ins.2010.03.016.

Wan, L., Zeiler, M., Zhang, S., Le Cun, Y., and Fergus, R. Regularization of neural networks using dropconnect. In *International Conference on Machine Learning*, pp. 1058–1066, 2013.

Wang, S. and Sun, X. Generalization of hinging hyperplanes. *IEEE Transactions on Information Theory*, 51(12):4425–4431, 2005.

Xiao, H., Rasul, K., and Vollgraf, R. Fashion-mnist: a novel image dataset for benchmarking machine learning algorithms. *arXiv preprint arXiv:1708.07747*, 2017.

Zamora, E. and Sossa, H. Dendrite morphological neurons trained by stochastic gradient descent. *Neurocomputing*, 260:420–431, October 2017. ISSN 0925-2312. doi: 10.1016/j.neucom.2017.04.044.

Supplementary Material of Dense Morphological Network: An Universal Function Approximator

Anonymous Authors¹

A. Proof of Lemma 1

where

$$\begin{aligned}\beta_i &= \begin{cases} \beta_i^+ & \text{if } i \leq n \\ \beta_{i-n}^- & \text{if } n < i \leq m+n \end{cases} \\ d_{ik} &= \begin{cases} d_{ik}^+ & \text{if } i \leq n \\ d_{(i-n)k}^- & \text{if } n < i \leq m+n \end{cases} \\ \alpha_i &= \begin{cases} \alpha_i^+ & \text{if } i \leq n \\ \alpha_{(i-n)}^- & \text{if } n < i \leq m+n \end{cases}\end{aligned}$$

Lemma 1 $g(\mathbf{x})$ is sum of multi-order hinge functions.

From equation 6 we have

$$g(\mathbf{x}) = \sum_{i=1}^n \omega_i^+ z_i^+ + \sum_{j=1}^m \omega_j^- z_j^- \quad (1)$$

Now this equation can be rewritten as follows

$$g(\mathbf{x}) = \sum_{i=1}^n \omega_i^+ \max_k (x_k + s_{ik}^+) + \sum_{i=1}^m -\omega_i^- \max_k (s_{ik}^- - x_k), \quad (2)$$

where s_{ik}^+ and s_{ik}^- denote the k^{th} component of the i^{th} structuring element of dilation and erosion neurons, respectively. The above equation can be further expressed in the following form,

$$g(\mathbf{x}) = \sum_{i=1}^n \alpha_i^+ \max_k (\beta_i^+ x_k + d_{ik}^+) + \sum_{i=1}^m \alpha_i^- \max_k (\beta_i^- x_k + d_{ik}^-). \quad (3)$$

Where β_i^+ , β_i^- , d_{ik}^+ and d_{ik}^- are define in the following way

$$\begin{aligned}\beta_i^+ &= \begin{cases} \omega_i^+ & \text{if } \omega_i^+ \geq 0 \\ -\omega_i^+ & \text{if } \omega_i^+ < 0 \end{cases} & \beta_i^- &= \begin{cases} -\omega_i^- & \text{if } \omega_i^- \geq 0 \\ \omega_i^- & \text{if } \omega_i^- < 0 \end{cases} \\ d_{ik}^+ &= \begin{cases} s_{ik}^+ \omega_i^+ & \text{if } \omega_i^+ \geq 0 \\ -s_{ik}^+ \omega_i^+ & \text{if } \omega_i^+ < 0 \end{cases} & d_{ik}^- &= \begin{cases} s_{ik}^- \omega_i^- & \text{if } \omega_i^- \geq 0 \\ -s_{ik}^- \omega_i^- & \text{if } \omega_i^- < 0 \end{cases} \\ \alpha_i^+ &= \begin{cases} 1 & \text{if } \omega_i^+ \geq 0 \\ -1 & \text{if } \omega_i^+ < 0 \end{cases} & \alpha_i^- &= \begin{cases} -1 & \text{if } \omega_i^- \geq 0 \\ 1 & \text{if } \omega_i^- < 0 \end{cases}\end{aligned}$$

Now, without any loss of generality we can write equation 3 as follows

$$g(\mathbf{x}) = \sum_{i=1}^{m+n} \alpha_i \max_k (\beta_i x_k + d_{ik}) \quad (4)$$

¹Anonymous Institution, Anonymous City, Anonymous Region, Anonymous Country. Correspondence to: Anonymous Author <anon.email@domain.com>.

Preliminary work. Under review by the International Conference on Machine Learning (ICML). Do not distribute.

Finally, we can rewrite equation 4 as

$$g(\mathbf{x}) = \sum_{i=1}^l \alpha_i \phi_i(\mathbf{x}), \quad (5)$$

where $l = m + n$, $\alpha_i \in \{1, -1\}$ and $\phi_i(\mathbf{x})$'s are of the following form

$$\phi_i(\mathbf{x}) = \max_k (\mathbf{v}_{ik}^T \mathbf{x} + d_{ik}), \quad (6)$$

with

$$\mathbf{v}_{ikt} = \begin{cases} \beta_i & \text{if } t = k \\ 0 & \text{if } t \neq k \end{cases} \quad (7)$$

In equation 6, $\mathbf{v}_{ik}^T \mathbf{x} + d_{ik}$ is affine and $\alpha_i \phi_i(\mathbf{x})$ is a d -order hinge function. Hence $\sum_{i=1}^l \alpha_i \phi_i(\mathbf{x})$ i.e., $g(\mathbf{x})$ represents sum of multi-order hinge function.

However, it may be noted that taking $l \geq d$ results hinge hyper planes which can span any where in d dimensional input space. We can assume there are l_1 and l_2 number of terms where $\alpha = 1$ and $\alpha = -1$ respectively, then

$$g(\mathbf{x}) = \sum_{i=1}^{l_1} \phi_i'(\mathbf{x}) - \sum_{i=1}^{l_2} \phi_i''(\mathbf{x}), \quad (8)$$

where $l_1 + l_2 = l$ and $\phi_i'(\mathbf{x}), \phi_i''(\mathbf{x})$ is of same form as equation 6. Therefore can write,

$$\sum_{i=1}^{l_1} \phi_i'(\mathbf{x}) = \sum_{i=1}^{l_1} \max_k (\mathbf{v}_{ik}^T \mathbf{x} + d_{ik}), \quad (9)$$

055
056 $\sum_{i=1}^{l_1} \phi_i'(\mathbf{x}) = \max_{k_1, k_2, k_3, \dots, k_{l_1}} \left(\sum_{i=1}^{l_1} \mathbf{v}_{ik_i} \right)^T \mathbf{x} + \sum_{i=1}^{l_1} d_{ik_i} \right) \quad (10)$
057

058 where $k_i \in \{1, 2, \dots, d+1\} \forall i$. In equation 10 we are taking
059 maximum of $(d+1)^{l_1}$ terms. Similarly we can derive same
060 expression for $\sum_{i=1}^{l_2} \phi_i''(\mathbf{x})$. Hence out of all l number of
061 sum we can select d number of coefficient of \mathbf{x} . So, $l \geq d$
062 results in hinge hyperplanes which can span any where in
063 d -dimensional space.

B. Alternative theoretical justification

064
065 Here give an alternate proof of the claim that $g(\mathbf{x})$ can
066 approximate any continuous function. For that take the help
067 of following two proposition.

068 **Proposition 1 (From ?)** *Any continuous piece-wise linear*
069 *function (PWL) can be expressed by as difference of two*
070 *convex PWL function.*

071 Then we show the following,

072 **Lemma 2** *$g(\mathbf{x})$ is a continuous piece-wise linear function.*

073 **Proof** From equation 5, without any loss of generality we
074 can assume there are t_1 and t_2 number of terms where $\alpha = 1$
075 and $\alpha = -1$ respectively, then

076
077
$$g(\mathbf{x}) = \sum_{i=1}^{t_1} \phi_i'(\mathbf{x}) - \sum_{i=1}^{t_2} \phi_i''(\mathbf{x}), \quad (11)$$

078

079 where $t_1 + t_2 = l$ and $\phi_i'(\mathbf{x}), \phi_i''(\mathbf{x})$ are of same form as
080 equation 6.

081 As sum of PWL functions is also a PWL function, hence
082 each $\sum_{i=1}^{t_1} \phi_i'(\mathbf{x})$ and $\sum_{i=1}^{t_2} \phi_i''(\mathbf{x})$ and PWL. Now, if
083 $t_1 > 0$, from Proposition 1 we can conclude that $g(\mathbf{x})$ is
084 PWL linear function since difference of two continuous
085 PWL function is PWL function. If $t_1 = 0$ then $g(\mathbf{x})$ becomes
086 PWL concave function. Hence, can say $g(\mathbf{x})$ is PWL
087 function.

088 It may be noted that if $l < d$ then PWL hyperplane will be in
089 parallel to at least one of the axis. Taking $l \geq d$ results PWL
090 hyperplane which may span anywhere in d dimensional
091 space.

092 **Theorem 1 (Universal approximation)** *Using only a single*
093 *dilation-erosion layer followed by a linear combination*
094 *layer any continuous function can be approximated.*

095 **Sketch of Proof** From Stone-Weierstrass approximation
096 theorem we get that any continuous function can be well
097 approximated by a PWL function with an error bound of
098 ϵ . Now from lemma 2 we know that our DenMo-Net with
099 of n dilation and m erosion neurons followed by a linear

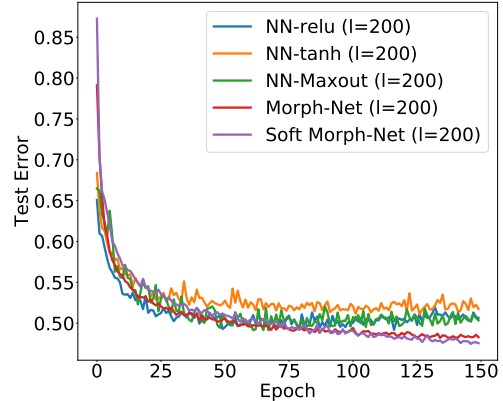


Figure 1. Epochs vs test error of different networks with 200 hidden nodes in CIFAR10.

combination layer computes a PWL function. Hence we can say our network can approximate any continuous function. In general if we increase the neurons in the dilation-erosion layer, number of affine function in $g(\mathbf{x})$ (equation 4) increases and the error bound $\epsilon \rightarrow 0$.

C. Proof of Soft Maximum

Let $a_k = x'_k + s_k$

$$\mathbf{x} \oplus \mathbf{s} = \lim_{\beta \rightarrow \infty} \log(\sum_k e^{a_k \beta}) / \beta \quad (12)$$

Applying L'Hospital's Rule, we get

$$\begin{aligned} &= \lim_{\beta \rightarrow \infty} \frac{\sum_k a_k e^{a_k \beta}}{\sum_k e^{a_k \beta}} \\ &= \lim_{\beta \rightarrow \infty} \sum_j \frac{a_j e^{a_j \beta}}{\sum_k e^{a_k \beta}} \\ &= \lim_{\beta \rightarrow \infty} \sum_j \frac{a_j}{1 + \sum_{k \neq j} e^{(a_k - a_j) \beta}} \\ &= \sum_j \lim_{\beta \rightarrow \infty} \frac{a_j}{1 + \sum_{k \neq j} e^{(a_k - a_j) \beta}} \\ &= \max_j a_j \end{aligned} \quad (13)$$

D. CIFAR 10 Experiments

We have shown the learning graph over epochs on CIFAR10 dataset with different hidden neurons. It may be noted, for Soft DenMo-Net we have taken $\beta = 12$

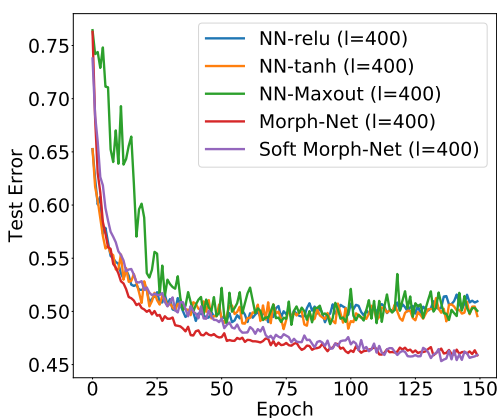


Figure 2. Epochs vs test error of different networks with 400 hidden nodes in CIFAR10.

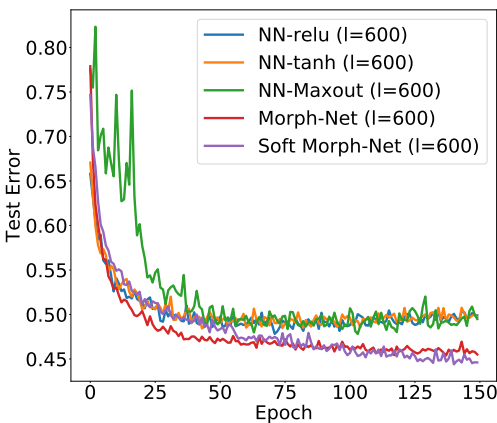


Figure 3. Epochs vs test error of different networks with 600 hidden nodes in CIFAR10.

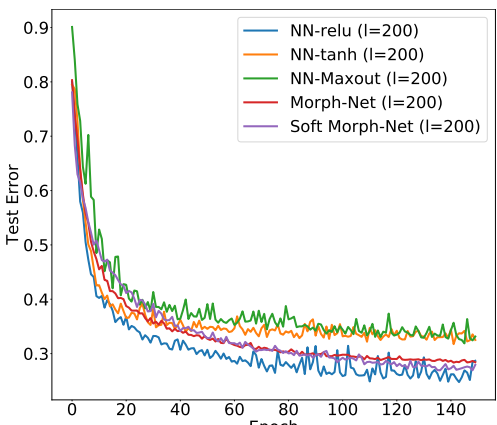


Figure 4. Epochs vs test error of different networks with 200 hidden nodes in SVHN.

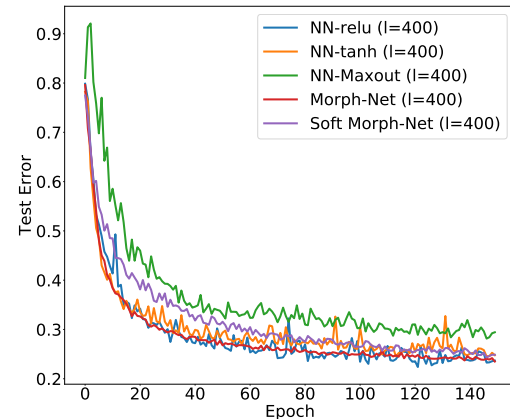


Figure 5. Epochs vs test error of different networks with 400 hidden nodes in SVHN.

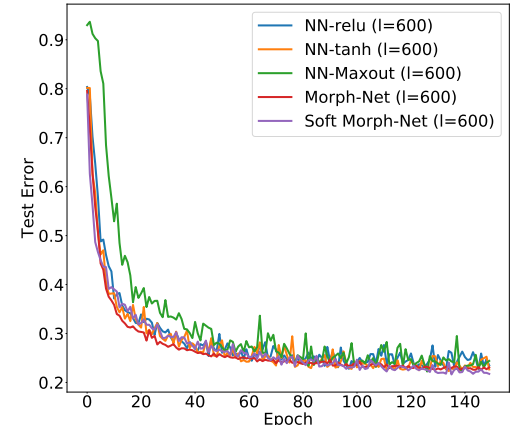


Figure 6. Epochs vs test error of different networks with 600 hidden nodes in SVHN.

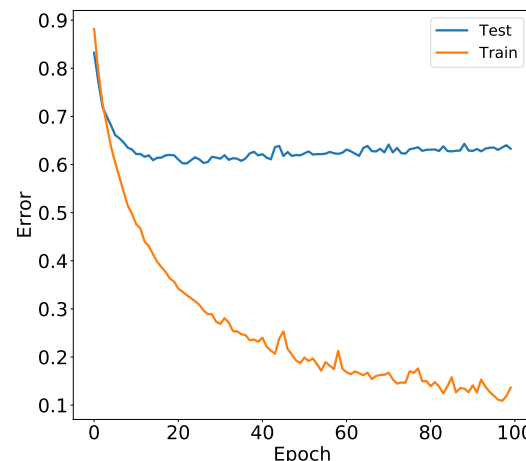


Figure 7. Epochs vs training and test error in cifar10 with network architecture 200DE-200FC-200DE-10FC. The network highly over fits the cifar10 data. The training error decreases over the epochs, whereas test error is more or less same over the epochs